# Open Circuit Fault Diagnosis Strategy for a Generalized $n$-Levels CHB Multilevel Converters

**K.O. Mtepele, J.A. Pecina-Sánchez, D.U. Campos-Delgado, A.A. Valdez-Fernández**

*Facultad de Ciencias, Universidad Autónoma de San Luís Potosí, San Luís Potosí, México (e-mail: mtepele@gmail.com, angel.pecina@alumnos.uaslp.edu.mx, ducd@fciencias.uaslp.mx, andres.valdez@ieee.org)*

**Abstract:** Safe operation of power conversion devices is an important property in various industrial and domestic applications. This paper aims to define a comprehensive model-based fault diagnosis strategy for open-circuit faults (OCFs) in the switching devices of a cascade H-bridge converter with $n$-levels (CHB-$n$L). The application of the CHB-$n$L converter as a single-phase active filter is focused. The OCFs are modeled as additive voltage profiles into the subsystems describing the dynamics of each H-bridge in the converter, where each fault profile is identified by a constant component plus an oscillatory term. The diagnosis task is performed by suggesting a nonlinear sliding-mode proportional-integral (PI) observer to estimate the OCF profiles, independently of the operating point of the converter. Based on the estimated constant components, fault detection and isolation is achieved. Furthermore, no additional sensors are needed to carry out the diagnosis media besides the ones usually used for control purposes. To validate the ideas proposed in this work, a simulation evaluation is carried out under a single OCF condition.

*Keywords:* Fault diagnosis, open-circuit faults, multilevel converter, sliding-mode observer.

## 1. INTRODUCTION

The increasing use of power electronics-based loads (adjustable speed drives, switch mode powersupplies, among others), and the necessity of producing higher power quality waveforms has led several power research groups to focus on the study, design, control, and applications of multilevel converter topologies (Escobar et al., 2013)-(Valdez et al., 2013). In industrial applications and alternative energy systems, cascade H-bridge (CHB) multilevel converters have been largely studied by its scalability, feasibility, reliability and modularity (Marks et al., 2014)-(Townsend et al., 2016). A series connection of single-phase H-bridge converters with separated DC buses is employed in a CHB multilevel converter. However, both an adequate modulation algorithm and a control strategy must be jointly applied to correctly exploit the advantages of CHB multilevel converters (Dell'Aquila et al., 2008). In this scenario, a good knowledge of a mathematical model of the system dynamics (Dell'Aquila et al., 2008) is a key step of a successful application. This dynamic model can be further employed in a model-based fault detection and isolation (FDI) strategy (Sim et al., 2013), (Isermann, 2006).

In this context, novel active power filters rely on the advantages of multilevel topologies to achieve a high performance, but at the expense of a large number of semiconductor devices (Escobar et al., 2013). Nonetheless, the probability of a fault in multilevel converters is raised by the number of semiconductors employed in the topology (Townsend et al., 2014)-(Wang et al., 2013). As has been documented in previous studies from the literature (Choi et al., 2015), a high percentage of faults occurs in the switching devices of the multilevel converters, which can be classified in two groups: open-circuit and short-circuit faults (OCFs and SCFs). However, under appropriate passive protections in the power converter topology, these two classes have the same electrical symptoms and can be treated with similar diagnostic algorithms (Wu et al., 2013; Espinoza-Trejo and Campos-Delgado, 2011; Wang et al., 2015).

In the literature, the diagnosis of OCF in multilevel converter have studied by several research groups. In (Riera-Gusp et al., 2015), an analysis of the state of the art in electrical machines fault diagnosis and drives condition monitoring is presented. Furthermore, Choi et al. (2015) provided an overview of the failure mechanisms in IGBTs modules and their handling methods. Caseiro et al. (2015) proposed a fault diagnosis algorithm based on the analysis of the instant pole voltage of a neutral-point-clamped UPS inverter. Meanwhile, a fault diagnosis and fault tolerant method for SCF in cascade half-bridge inverters based on a model-based approach was suggested by Alavi et al. (2015). In (Ouni et al., 2015), a method to detect the faulty cell in a CHB inverter is proposed by comparing the output voltage with a reference one synthetized by the control states of the switches and DC-link voltage. On the other hand, Wang et al. (2015) employed principal component

analysis and a multiclass relevance vector machine to diagnosis an OCF, where the fast Fourier transform of the output voltages signals provides distinct features to perform the classification strategy. In a recent proposal, Sim et al. (2013) introduced a method to detect faulty cells in CHB multilevel inverters, where an OCF condition is first recognized by evaluating the slope of the current trajectory. Next, the isolation stage is carried out by analyzing the current trajectory during the zero-voltage switching states.

In this context, the main contribution of this paper is a new methodology for model-based FDI of OCFs in a single-phase CHB multilevel converter, for the general case of $n$-levels (CHB-$n$L) obtained by $N$ H-bridges. The CHB-$n$L converter as a shunt active filter is studied, and as a consequence, the generalized model for the whole system is obtained. Departing from the system description, the OCFs are modeled as additive voltage signals into each subsystem of the multilevel converter. Due to the dynamic structure of the model, a global proportional-integral (PI) observer is suggested to detect and isolate the OCFs by using a sliding-mode philosophy. For validation purposes, the FDI strategy is simulated under a closed-loop operation of the shunt active filter. This work extends our previous effort in (Mtepele et al., 2016) by using a new perspective for the fault modeling, a sliding mode methodology for the observer, and a centralized structure for the diagnostics to improve the fault robustness and sensitivity.

The rest of the paper is organized as follows. Section 2 provides a description of the three-phase CHB-$n$L converter used in this work, and introduces its mathematical model and the control philosophy for the shunt active filter operation. The fault modeling for OCFs, the residual generation based on sliding-mode PI nonlinear observers, and the proposed fault detection and isolation schemes are detailed in Section 3. In Section 4, the simulation evaluation of the new FDI scheme is illustrated based on a CHBs topology of seven-levels, and finally concluding remarks are described in Section 5.

## 2. CHB MULTILEVEL CONVERTER

Figure 1 shows the general structure of the studied CHB-$n$L converter used as shunt active filter in this research work. The generalized model of the system represented in Fig. 1 can be obtained by the application of Kirchhoff's law. This procedure yields the following average model of the system dynamics

$$L\frac{di}{dt} = v_S - \sum_{j=1}^{N} u_j v_{Cj}, \tag{1}$$

$$C\frac{dv_{Cj}}{dt} = u_j i - \frac{v_{Cj}}{R} \quad j \in \{1,\dots,N\}, \tag{2}$$

$$i_S = i + i_0, \tag{3}$$

where $v_S$ denotes the voltage at the point of common coupling (PCC), also referred as the grid voltage, $i_S$ is the grid current, $i$ is the injected current, $i_0$ is the distorted load current consumed by the nonlinear load (NLL); $v_{Cj}$ is the capacitor voltage in the DC bus of the $j$-th H-bridge, and $u_j \in [-1, 1]$ the corresponding duty cycle. Parameter $L$ is the input inductor for the active filter, $C$ is the capacitance in the DC buses, and $R$ is the resistor that models the losses in each H-bridge. For more details on the mathematical modeling, a reader may refer to (Valdez et al., 2015).

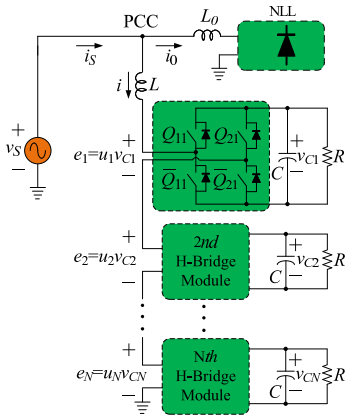


Fig. 1. Single-phase CHB-$n$L converter used as shunt active filter.

Based on the structure of the previous generalized model, a nominal controller was presented in Valdez et al. (2015). This controller consists of three feedback loops: a current tracking loop, a voltage regulation loop and $N-1$ voltage balance loops. The first one was composed of a damping term plus a bank of harmonic oscillators tuned at the harmonics of interest. The voltage regulation loop consisted of a conventional PI controller with limited bandwidth, so that the DC buses in the H-bridges are fixed, in average, at a constant value $V_d$. To achieve voltage balancing, $N-1$ control laws are synthesized as amplitude-modulated signals proportional to the fundamental component of the grid voltage, where the modulating gains are obtained by conventional PI control laws. A current reference proportional to the fundamental component of the grid voltage was used to guarantee an almost pure sinusoidal grid current. In this work, the injected current $i$, and the DC link voltages $v_{Cj}$ are assumed to be known variables available for both control and fault diagnosis purposes (Valdez et al., 2015).

## 3. FAULT DIAGNOSIS

The model described by (1) is employed for the synthesis of the dedicated sliding-mode observers in the model-based FDI proposal. Therefore, these observers are used for the detection and isolation of the OCFs in the switching devices of the CHB-$n$L converter. For this purpose, only the measurements of the injected current $i$ and capacitor voltages $v_{Cj}$ are necessary to implement the diagnosis media.

### *3.1 Fault Modeling in the CHB-nL Converter*

Once an OCF scenario occurs, the effect of this fault is suddenly reflected in the performance and efficiency of the CHB-$n$L converter, which is directly associated with a reduction of its voltage gain. This consideration allow us to model the converter faults by using an additive structure (Espinoza-Trejo and Campos-Delgado, 2011). In this way, the $j$-th faulty actuator signal $u_j^f(t)$ is modeled as

$$u_j^f(t) = u(t) + f_j(t) \quad j \in \{1, \ldots, N\}, \tag{4}$$

where $f_j(t)$ represents the induced fault profile by the $j$-th H-bridge. When the OCF occurs in the switching devices $Q_{1j}$ or/and $\bar{Q}_{2j}$, the $j$-th H-bridge is not able to supply the positive state of the output voltage $u_j v_{Cj}$. This leads to a fault profile $f_j$ that exhibits a negative direction, i.e. $f_j<0$. On the other hand, when the OCF occurs in switches $\bar{Q}_{1j}$ or/and $Q_{2j}$, now the $j$-th H-bridge is not able to supply the negative state of the output voltage. As a result, the positive profile is induced by this type of fault, i.e. $f_j>0$.

Similarly to the analysis performed in Pecina et al. (2013) and due the switching strategy in the CHB-$n$L converter, the pattern described by the $j$-th faulty actuator $u_j^f(t)$ will be periodic, and as a consequence, it will present a DC component plus harmonic components of the fundamental frequency in the converter. In fact, the DC component will be a distinctive characteristic of the OCFs present in the converter. Therefore the total fault profile induced by the $j$-th faulty H-bridge can be expressed as

$$f_j(t) = f_j^{DC} + f_j^{OSC}(t) \quad j \in \{1, \ldots, N\}, \tag{5}$$

where $f_j^{DC}$ denotes the DC term and $f_j^{OSC}(t)$ is the oscillatory component. Hence the proposed FDI scheme can be focused just on evaluating $f_j^{DC}$ by the next following reasoning:

**Fault Detection:** A fault will induce an asymmetric actuator signal where $f_j^{DC} \neq 0$,

**Fault Isolation:** The faulty pair of switches in the H-bridge can be isolated by the pattern: (i) $(Q_{1j}, \bar{Q}_{2j})$ if $f_j^{DC} < 0$, and (ii) $(\bar{Q}_{1j}, Q_{2j})$ if $f_j^{DC} > 0$.

In fact, due to the structure of the CHB-$n$L converter, the oscillatory components in the fault profiles $f_j(t)$ are always bounded signals, i.e. $\exists \Gamma > 0$ such that $|f_j^{OSC}(t)| < \Gamma \ \forall t, j$.

### *3.2 Residual Generation by Model-Based Approach*

As described earlier, the proposed FDI scheme for OCFs relies on a model-based approach through dynamic observer design. In the literature, several approaches have been proposed for system observation (Isermann, 2006). The PI observer is one of the dynamical structures for state observation widely used due to their simplicity and capability to reject or estimate certain perturbations (Perruquetti and Barbot , 2002), (Espinoza-Trejo and Campos-Delgado, 2011). Consequently, the dynamic structure of the PI observer is suggested to reconstruct the state dynamics and generate an estimation of the fault profiles. From (2), the faulty model of shunt active filter can be expressed as

$$\begin{aligned} L\frac{di}{dt} &= v_S - \sum_{j=1}^{N}(u_j + f_j)v_{Cj}, \\ C\dot{v}_{Cj} &= (u_j + f_j)i - \frac{1}{R}v_{Cj} \quad j \in \{1, \ldots, N\}. \end{aligned} \tag{6}$$

From the previous model and as expected, $j$-th faulty actuator $u_j^f(t)$ modifies the overall injected current $i$ dynamics, as well as, the capacitor voltage time profile for its H-bridge. Hence, the fault profile generates coupling among the injected currrent and capacitor voltage dynamics in the shunt active filter. For this reason, we propose to build a global sliding-mode PI nonlinear observer for the states and the fault profiles estimation, based only on the information from the capacitor voltages $v_{Cj}$ and the injected current $i$, i.e., there is no need of additional measurements (sensors).

**Proposition**: The dynamical structure of the global sliding-mode PI nonlinear observer for FDI purposes is conformed by a copy of each subsystem in (6) plus linear and nonlinear correction terms, and an augmented state $\hat{f}_j$ to ensure the estimation of the DC fault profile:

$$\begin{aligned} L\frac{d\hat{i}}{dt} &= v_S - \sum_{j=1}^{N}(u_j + \hat{f}_j)v_{Cj} + K_i(i - \hat{i}) \\ &\quad + M_i|i - \hat{i}|^2 \operatorname{sign}(i - \hat{i}), \\ C\dot{\hat{v}}_{Cj} &= -\frac{1}{R}\hat{v}_{Cj} + (u_j + \hat{f}_j)i + K_v(v_{Cj} - \hat{v}_{Cj}) \\ &\quad + M_v|v_{Cj} - \hat{v}_{Cj}|^2 \operatorname{sign}(v_{Cj} - \hat{v}_{Cj}), \\ \dot{\hat{f}}_j &= K_f\left(i(v_{Cj} - \hat{v}_{Cj}) - v_{Cj}(i - \hat{i})\right) \quad j \in \{1, \ldots, N\}, \end{aligned} \tag{7}$$

where for simplicity the positive gains $(K_i, M_i, K_v, M_v, K_f)$ are common to all observers and $K_f > 0$ affects the desired convergence rate of the estimation. With this observer, the estimation errors in the injected current and capacitor voltages are bounded to a neighbourhood of the origin, and the error in the DC fault profile is also bounded.

**Proof**: First, the error functions are defined as

$$\begin{aligned} e_i &\triangleq i - \hat{i}, \\ e_{v_{Cj}} &\triangleq v_{Cj} - \hat{v}_{Cj}, \\ e_{fj} &\triangleq f_j^{DC} - \hat{f}_j. \end{aligned}$$

Next, from systems in (6) and (7), the time derivative along the error functions leads to the following error dynamic model:

$$\begin{aligned} L\dot{e}_i &= -K_i e_i - M_i|e_i|^2 \operatorname{sign}(e_i) - \sum_{j=1}^{N}(e_{fj} + f_j^{OSC})v_{Cj}, \\ C\dot{e}_{v_{Cj}} &= -\alpha_v e_{v_{Cj}} - M_v|e_{v_{Cj}}|^2 \operatorname{sign}(e_{v_{Cj}}) + (e_{fj} + f_j^{OSC})i, \\ \dot{e}_{fj} &= -K_f\left(ie_{v_{Cj}} - v_{Cj}e_i,\right) \end{aligned} \tag{8}$$

where $\alpha_v \triangleq (K_v + 1/R) > 0$. Now based on the structure of (8), the following Lyapunov energy function is proposed to evaluate the error convergence:

$$V = \frac{L}{2}e_i^2 + \frac{C}{2}\sum_{j=1}^{N} e_{vCj}^2 + \frac{1}{2K_f}\sum_{j=1}^{N} e_{fj}^2. \tag{9}$$

Then, by recalling that any $x \in \mathbb{R}$ can be expressed as $x = |x|\operatorname{sign}(x)$, and that for any operating condition in the CHB-$n$L converter $\exists v_{max} > 0$ and $i_{max}$ such that

$$|v_{Cj}| \leq v_{max} \quad \wedge \quad |i| \leq i_{max} \quad \forall t,$$

the time derivative of the function $V$ along the error dynamics leads to:

$$\dot{V} = -K_i e_i^2 - M_i|e_i|^3 - \sum_{j=1}^{N} f_j^{OSC} v_{Cj} e_i - \alpha_v \sum_{j=1}^{N} e_{v_{Cj}}^2 - M_v \sum_{j=1}^{N} |e_{v_{Cj}}|^3 + \sum_{j=1}^{N} f_j^{OSC} i\, e_{v_{Cj}}, \tag{10}$$

Next by using the upper bounds on the oscillatory component of the fault profiles, the injected current and capacitor voltages, we obtain

$$\dot{V} \leq -K_i e_i^2 - M_i|e_i|^3 + \sum_{j=1}^{N} |f_j^{OSC}||v_{Cj}||e_i|, - \alpha_v \sum_{j=1}^{N} e_{v_{Cj}}^2 - M_v \sum_{j=1}^{N} |e_{v_{Cj}}|^3 + \sum_{j=1}^{N} |f_j^{OSC}||i|\,|e_{v_{Cj}}|, \tag{11}$$

$$\leq -K_i e_i^2 - M_i|e_i|^3 + \Gamma N v_{max}|e_i| - \alpha_v \sum_{j=1}^{N} e_{v_{Cj}}^2 - M_v \sum_{j=1}^{N} |e_{v_{Cj}}|^3 + \Gamma i_{max} \sum_{j=1}^{N} |e_{v_{Cj}}|. \tag{12}$$

and by reorganizing terms, we conclude that

$$\dot{V} \leq -|e_i| \left[M_i|e_i|^2 + K_i|e_i| - \Gamma v_{max} N\right] \tag{13}$$

$$- \sum_{j=1}^{N} |e_{v_{Cj}}| \left[M_v|e_{v_{Cj}}|^2 + \alpha_v|e_{v_{Cj}}| - \Gamma i_{max}\right]. \tag{14}$$

Hence we have $\dot{V} < 0$ as long as we jointly satisfy

$$M_i|e_i|^2 + K_i|e_i| - \Gamma v_{max} N > 0, \tag{15}$$

$$M_v|e_{v_{Cj}}|^2 + \alpha_v|e_{v_{Cj}}| - \Gamma i_{max} > 0.. \tag{16}$$

So, by recalling that $K_i > 0$, $M_i > 0$ and $K_v > 0$, the quadratic equations in (15) and (16) will have one positive and one negative root, and since $|e_i| \geq 0$ and $|e_{v_{Cj}}| \geq 0$, the convergence condition becomes

$$|e_i| - \underbrace{\left(\frac{-K_i + \sqrt{K_i^2 + 4\Gamma v_{max} N M_i}}{2M_i}\right)}_{e_i^{max}} > 0, \tag{17}$$

$$|e_{v_{Cj}}| - \underbrace{\left(\frac{-\alpha_v + \sqrt{\alpha_v^2 + 4\Gamma i_{max} M_v}}{2M_v}\right)}_{e_v^{max}} > 0. \tag{18}$$

If we define the estimation error vector as

$$\mathbf{e} \triangleq [e_i \;\; e_{v_{C1}} \;\; \dots \;\; e_{v_{CN}}]^\top \in \mathbb{R}^{N+1}.$$

we obtain that $\dot{V} < 0$ if $\mathbf{e} \in \Omega$, where

$$\Omega = \left\{\mathbf{e} \mid |e_i| > e_i^{max} \;\wedge\; |e_{v_{Cj}}| > e_v^{max}\; j \in \{1, \dots, N\}\right\},$$

i.e. the Lyapunov function $V$ will decrease as long as the error vector $\mathbf{e}$ remains outside the set $\Omega$, and by the continuous dependence of $e_{fj}$ on $V$, the errors $e_{fj}$ will be bounded signals. Nonetheless, if the oscillatory component of the fault is absent, i.e. $f_j^{OSC} = 0$ or $\Gamma = 0$, then the convergence of $\mathbf{e}$ and $e_{fj}$ are guaranteed by La Salle's Principle (Khalil, 1996). ■

Two important remarks can be outlined about the properties of the sliding-mode PI nonlinear observer in (7):

- The observer gains $(K_i, M_i, K_v, M_v, K_f)$ does not depend on the model parameters of the CHB-$n$L converter.
- The control gains $M_i$ and $M_v$ in the sliding-mode correction terms will affect the upper bounds $e_i^{max}$ and $e_v^{max}$ of the convergence neighbourhood, i.e. if $M_i$ and $M_v$ increase, the upper bounds $e_i^{max}$ and $e_v^{max}$ will be reduced, but the effect of the measurement noise will be increased.

### *3.3 Fault Detection and Isolation*

From the sliding-mode PI nonlinear observers in (7), the DC components of the fault profiles $f_j^{DC}$ are estimated by $\hat{f}_j$. Due to the rapid variations of the injected current $i$ (Valdez et al., 2015), the estimations $\hat{f}_j$ could have oscillatory components, so in order to obtain a pure DC term, from the estimated total fault profile $\hat{f}_j$, the following moving average is calculated

$$\hat{f}_j^{DC} = \frac{1}{T}\int_{t-T}^{T} \hat{f}_j(t)dt \quad j \in \{1, \dots, N\}. \tag{19}$$

where $T$ is the period of the supply voltage $v_S$. Next, following the discussion in Section 2.1, the residuals $r_j$ are formulated by taking into account the uncertainty in the estimations as

$$r_j = \begin{cases} \hat{f}^{DC}, & |\hat{f}^{DC}| > J_{TH} \\ 0, & |\hat{f}^{DC}| \leq J_{TH} \end{cases} \quad j \in \{1, \dots, N\}. \tag{20}$$

where $J_{TH} > 0$ is a threshold parameter. Hence, we introduce $J_{TH}$ to take into account measurement noise, as well as, high frequency switching in the CHB-$n$L converter. Regarding this parameter, the corresponding value can be set by running the system under a free-fault scenario such that

$$J_{TH} = \max_{no\ fault, \forall t, j} |\hat{f}_j^{DC}(t)|. \tag{21}$$

Therefore, fault detection task is accomplished if

$$\text{Fault Decision} = \begin{cases} \text{Fault}, & |r_j| > 0 \\ \text{No Fault}, & |r_j| = 0 \end{cases} \quad \forall j. \tag{22}$$

Once a fault is detected, the sign of the fault residuals $r_j$ is evaluated so that the faulty H-bridge is isolated.

## 4. SIMULATION RESULTS

In order to evaluate the OCF diagnosis strategies addressed in this paper, the simulation of an active power filter based on a seven-levels cascade H-bridge converter (CHB-7L) topology with $N = 3$ H-bridges is presented in this section. A voltage source of 127 $V_{RMS}$ and supply frequency $f_0 = 60$ Hz ($T = 1/60$ s=16.67 ms and $\omega_0 = 2\pi f_o$ rad/s) is used. A single-phase diode bridge rectifier is considered as the nonlinear load that includes a smoothing inductor of $L_0 = 0.1$ mH, DC capacitor of $C_0 = 87$ $\mu$F, where its resistive load was changed from $R_0 = 50\ \Omega$ to $R_0 = 100\ \Omega$ and then back to $R_0 = 50\ \Omega$ to simulate a load change during the interval $0.6 \leq t \leq 0.85$ s. The active filter has been designed with parameters $L = 3.6$ mH and $C = 2200$ $\mu$F. The voltage reference for the DC capacitors is fixed to $V_d = 70$ V. The controller scheme has been implemented in Simulink/MatLab, where

a sampling frequency of $f_s = 30$ kHz is used. A phase-shifted multi-carrier modulation technique has been employed to generate the switching sequences for the IGBTs. This switching frequency is fixed to $f_{sw} = 5$ kHz, which produces an effective converter pulsating frequency of 30 kHz.

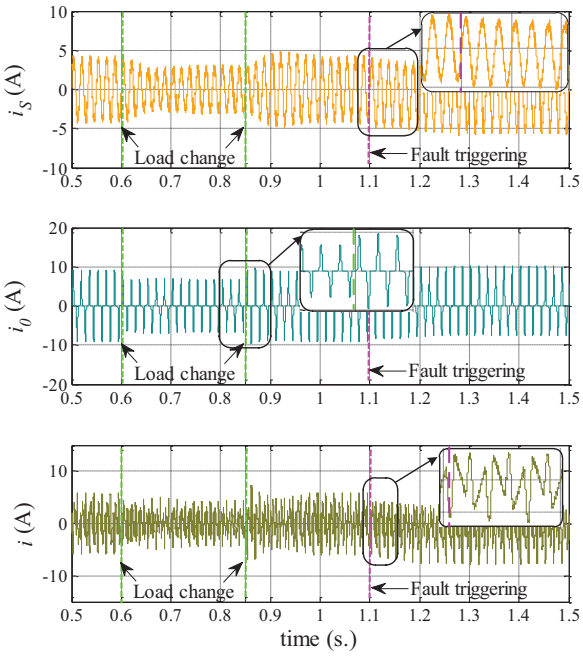


Fig. 2. Transient response of the active filter under the proposed solution during load step changes.

After attaining the steady state response, a disturbance (step load change) is induced to the system, and later on, an OCF fault is induced at $t = 1.1$ s in the first H-bridge of the converter, specifically in the switches $(Q_{11}, \bar{Q}_{21})$. In this case, the threshold value in (20) was fixed to $J_{TH} = 0.5$, which was selected by observing the system in a free fault condition, and measuring the peak value in the estimations.

Figure 2 illustrates, for the proposed solution, the transient responses of the CHB-7L topology based active filter during step changes of the load resistor going from $R_0 = 100\ \Omega$ to $R_0 = 50\ \Omega$ and back to $R_0 = 100\ \Omega$, and then, during the OCF scenario. The illustrated signals are: (from top to bottom) compensated grid current $i_S$, load current $i_0$ and injected current $i$. Notice that, during the load change, the envelopes of all currents reach constant values after relatively short transients. In particular, the transient of the grid current $i_S$ is sufficiently smooth with a relatively small overshoot. In addition, after the fault scenario the compensated current $i_S$ is no longer sinusoidal. This situation indicates that the tracking objective is not being be fulfilled anymore.

For the same scenarios of Fig. 2, now Fig. 3 shows (top to bottom), the generated residuals $r_1$, $r_2$ and $r_3$ for the H-bridges 1, 2, and 3. Observe that, after the OCF scenario, the residual $r_1$ exceeds the threshold value $J_{TH}$ at $t = 1.1232$ s, i.e. only 23.2 ms are needed to detect the fault. Hence, the 1st H-bridge is classified as the faulty bridge, and since, $r_1$ is positive, an OCF in the switches $(\bar{Q}_{11}, Q_{21})$ by the discussion in Section 3.1. On the contrary, the residuals remain unaltered during the load change scenario during the interval $0.6 \leq t \leq 0.85$ s. Therefore the robustness of the FDI methodology proposed in this paper was tested successfully.

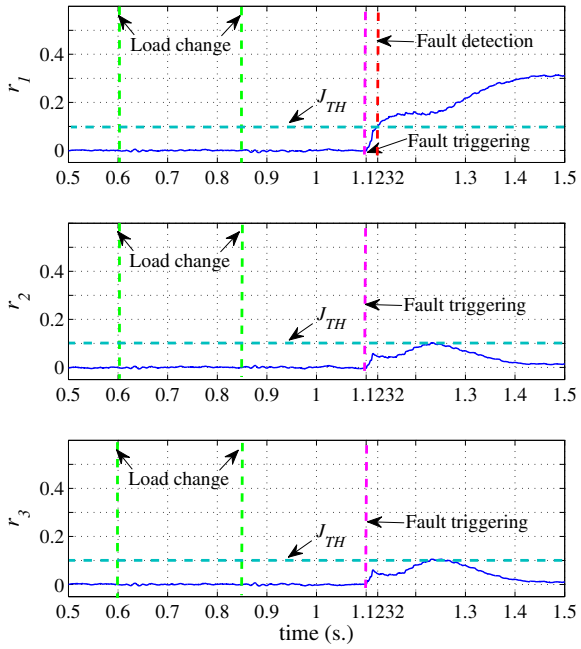


Fig. 3. The generated fault residuals $r_1$ (top), $r_2$ (middle) and $r_3$ (bottom) after an OCF in the 1st H-bridge.

Figure 4 depicts the transient responses of the capacitor voltages $v_{C1}$, $v_{C2}$ and $v_{C3}$ during the applied load change and OCF scenarios. Before and after the first scenario, the voltages are maintained at their reference value of $V_d = 70$ V. Moreover, once the OCF is detected, these capacitor voltages diverge from their constant reference indicating that the regulation and balance objectives are no longer achieved.

## 5. CONCLUDING REMARKS

This paper presented a generalized model-based fault diagnosis strategy for OCFs in the switching devices of a single-phase CHB-$n$L converter used as shunt active filter. In order to accomplish this goal, a sliding-mode PI nonlinear observer was suggested to estimate the fault profiles based on an additive fault model. These profiles were estimated to generate residuals that are independent of the operating point of the converter. As expected, the residuals were used for fault detection and isolation in the single-phase CHB-$n$L active filter. An important property of our proposal is that the diagnosis media was carried out without the need of additional sensors and the observers does not rely on the model parameters. To validate the ideas proposed in this work, the simulation study was carried out under a single OCF scenario (i.e. a fault in only one switch at a time). During our evaluation, the proposed FDI methodology only required at most one and a half-cycles of the fundamental frequency $f_0$. As

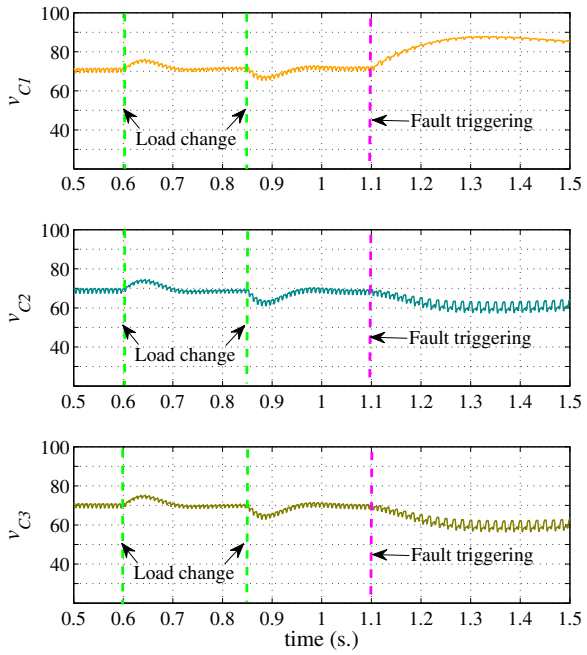


Fig. 4. The transient responses of the capacitor voltages $v_{C1}$ (top), $v_{C2}$ (middle) and $v_{C3}$ (bottom) when an OCF is triggered in switches $Q_{13}$ and/or $\bar{Q}_{23}$.

a future work, the present proposal has to be evaluated in an experimental test-bed under operating practical conditions.

## REFERENCES


M. Alavi, D. Wang, and M. Luo, Model-based Diagnosis and Fault Tolerant Control for Multi-Level Inverters. *In Proc. IECON 2015*, 1548-1553, Yokohama, Japan, 2015.

L.M.A. Caseiro, and A.M.S. Mendes, Open-Circuit Fault Diagnosis in Neutral-Point-Clamped UPS Inverters with no Additional Sensors. *In Proc. IECON 2015*, 2463-2468, Yokohama, Japan, 2015.

U.M. Choi, F. Blaabjerg, and K. B. Lee, Study and Handling Methods of Power IGBT Module Failures in Power Electronic Converter Systems. *IEEE Trans. Pow. Electron.*, 30:2517-2533, 2015.

A. Dell'Aquila, M. Liserre, V. G. Monopoli, and P. Rotondo, Overview of PI-based solutions for the control of DC buses of a single-phase H-bridge multilevel active rectifier. *IEEE Trans. Ind. Appl.*, 44:857-866, 2008.

G. Escobar, A. A. Valdez, M. F. Martinez-Montejano, and V. M. Rodriguez-Zermeno A model-based controller for the cascade multilevel converter used as a shunt active filter. *In Proc. Industry Applications Society.*, 10:1837-1843, Sep. 22-28, 2007.

D.R. Espinoza-Trejo and D.U. Campos-Delgado, An Observer-Based Faults Diagnosis for Single and Simultaneous Faults in Induction Motor Drives. *IEEE Trans. Ind. Electron.*, 58:671-679, 2011.

R. Isermann, *Fault-Diagnosis Systems: An Introduction from Fault Detection to Fault Tolerance*. Springer, 2006.

Z. Ji, J. Zhao, Y. Sun, X. Yao, and Z. Zhu, Fault-Tolerant Control of Cascaded H-Bridge Converters Using Double Zero-Sequence Voltage Injection and DC Voltage Optimization. *Journal of Power Electron.*, 14:946-956, 2014.

H.K. Khalil. *Nonlinear Systems*. 2nd Ed., Prentice Hall, 1996.

N. D. Marks, T. J. Summers, and R. E. Betz, Control of a 19 Level Cascaded H-bridge Multilevel Converter Photovoltaic System. *IEEE Energy Conversion Congress and Exposition (ECCE)*, 2265-22726, Pittsburgh, PA, Sept. 2014.

K. O. Mtepele, D. U. Campos-Delgado, A. Valdez-Fernandez and J. A. Pecina-Snchez, Fault tolerant controller for a generalized n-level CHB multilevel converter. *13th Int. Conf. on Power Electronics (CIEP)*, 75-80, Guanajuato, MX, 2016.

S. Ouni, J. Rodriguez, *et al.*, A Fast and Simple Method to Detect Short Circuit Fault in Cascade H-Bridge Multilevel Inverter. *In Proc. ICIT 2015*, 866-871, Seville, Spain, 2015.

J.A. Pecina-Sanchez, D.U. Campos-Delgado, D.R. Espinoza-Trejo, and E.R. Arce-Santana, Diagnosis of Open Switch Faults in Variable Speed Drives by Stator Current Analysis and Pattern Recognition. *IET Electric Pow. Appl.*, 7:509-522, 2013.

W. Perruquetti, and J.P. Barbot, *Slinding Mode Control In Engineering*. CRC Press, 2009.

M. Riera-Gusp, J. A. Antonino, and G. A. Capolinio, Advances in Electrical Machine, Power Electronic, and Drive Conditioning Monitoring and Fault Detection. *IEEE Trans. Ind. Electron.*, 62:1746-1759, 2015.

H.W. Sim, J.S. Lee, and K.B. Lee, Using asymmetric zero-voltage switching states Detection Open-Switch Faults. *IEEE Industry Appl. Magazine*, 22:27-37, April 2016.

C. D. Townsend, Y. Yu, G. Konstantinou, and V. G. Agelidis, Cascaded H-Bridge Multilevel PV Topology for Alleviation of Per-Phase Power Imbalances and Reduction of Second Harmonic Voltage Ripple. *IEEE Trans. Pow. Electron.*, 31:5574-5586, 2016.

C.D. Townsend, Y. Yu, G. Konstantinou, and V. G. Agelidis, Survey of Fault-Tolerance Techniques for Three-Phase Voltage Source Inverters. *IEEE Trans. Ind. Electron.*, 61:5192-5201, 2014.

A. A. Valdez-Fernández, K.O Mtepele, and D.U Campos-Delgado, A Generalized Model-Based Controller for the n-level CHB Multilevel Converter Used as a Shunt Active Filter. *IEEE Int. Autumn Meet. on Pow. Electron. and Comp. (ROPEC)*, Guerrero, MX, Nov. 2015.

A. A. Valdez-Fernández, P. R. Martínez-Rodríguez, G. Escobar, C. A. Limones-Pozos, and J. M. Sosa, A Model-Based Controller for the Cascade H-Bbridge Multilevel Converter Used as a Shunt Active Filter. *IEEE Trans. Ind. Electron.*, 60:5019-5028, 2013.

T. Wang, H. Xu, J. Han, H. Bouchikhi, and M. H. Benbouzid, Cascaded H-Bridge Multilevel Inverter System Fault Diagnosis Using a PCA and Multiclass Relevance Vector Machine Approach. *IEEE Trans. Pow. Electron.*, 30:7006-7018, 2015.

H. Wang, M. Liserre, and F. Blaabjerg, Toward Reliable Power Electronics: Challenges, Design Tools, and Opportunities. *IEEE Ind. Electron. Mag.*, 7:17-26, 2013.

R. Wu, F. Blaabjerg, H. Wang, M. Liserre, and F. Iannuzzo, Catastrophic Failure and Fault-Tolerant Design of IGBT Power Electronic Converters - An Overview. *In Proc. IECON 2013*, 507- 513, Vienna, 2013.